Cell Reports, Volume *32*

Supplemental Information

A Carbohydrate-Binding Protein from the Edible *Lablab* Beans Effectively Blocks the Infections of Influenza Viruses and SARS-CoV-2

Yo-Min Liu, Md. Shahed-Al-Mahmud, Xiaorui Chen, Ting-Hua Chen, Kuo-Shiang Liao, Jennifer M. Lo, Yi-Min Wu, Meng-Chiao Ho, Chung-Yi Wu, Chi-Huey Wong, Jia-Tsrong Jan, and Che Ma

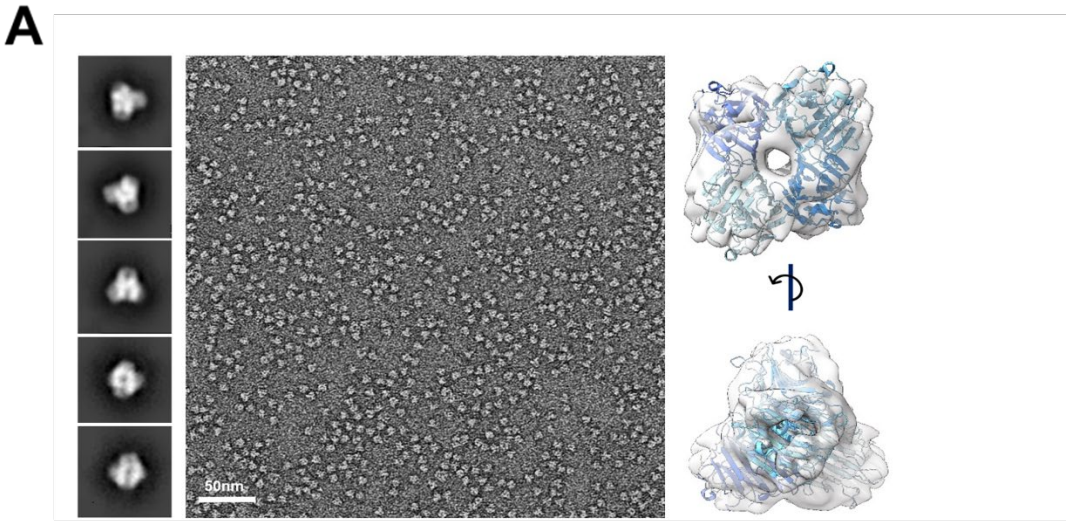

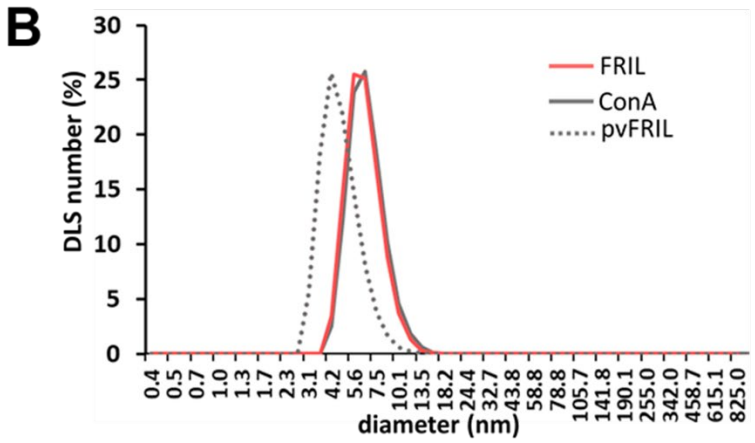

Figure S1. Isolation and characterization of FRIL, related to Figure 1. (A) Negative stain EM images of FRIL. Raw negative stain image (middle), representative 2D classes of FRIL (left) and 3D reconstructed FRIL density fitted with crystal structure (blue, PDB 1QMO) (right). **(B)** Dynamic light scattering size comparison of three related lectins: the tetrameric ConA (grey, from *Canavalia ensiformis*), FRIL (red, from *Lablab purpureus*) and pvFRIL (grey dotted, from *Phaseolus vulgaris*).

.

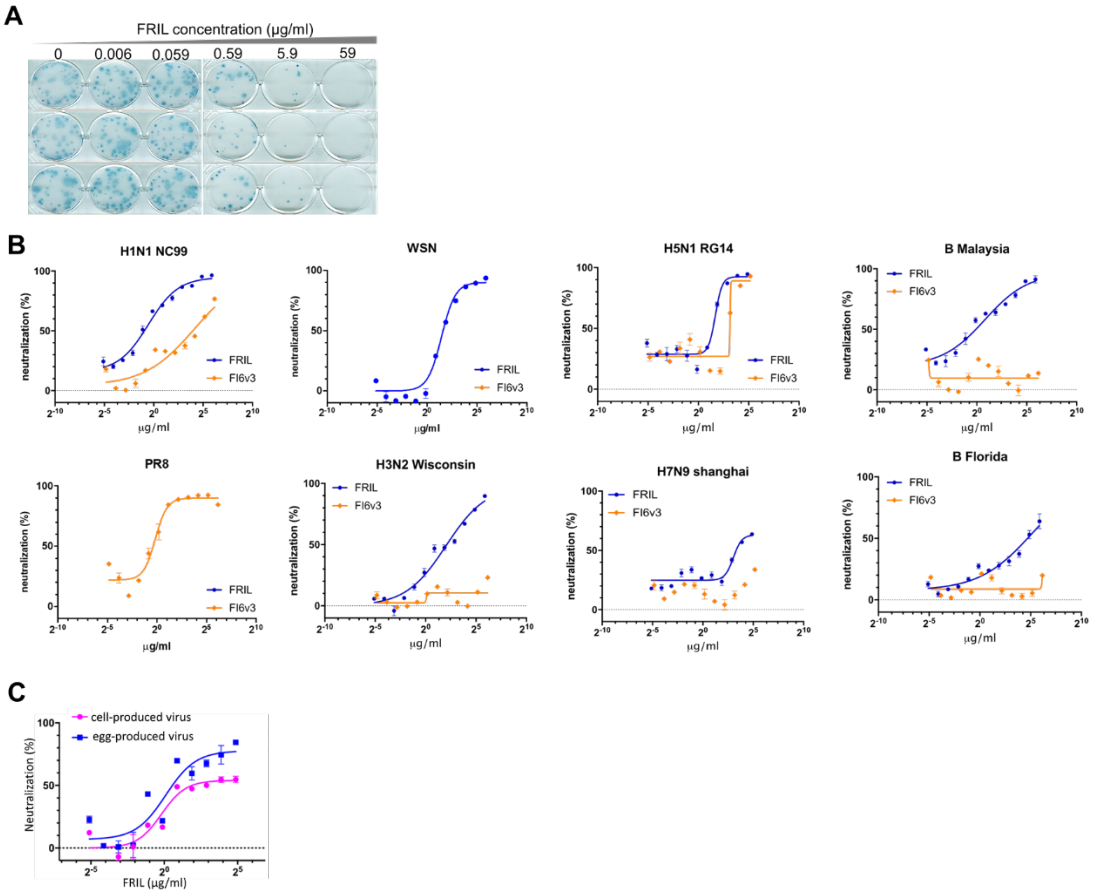

Figure S2. FRIL has anti-influenza activity, related to Figure 2. (A) Raw image of FRIL plaque reduction assay with H1N1 X181 (A/California/07/2009-like) virus, immunoplaques (blue) detected with anti-NP antibody. Plaque reduction curve presented in Fig. 2A. **(B)** MN of FRIL (blue) and bnAb FI6v3 (orange) were tested against H1N1 A/New Caledonia/20/99 (NC99), H1N1 A/WSN/33 (WSN), H1N1 A/PR/8/34 (PR8), H3N2 A/Wisconsin/67/2005-like, H5N1 A/Vietnam/1194/2004-like (RG14), H7N9 A/Shanghai/2/2013-like (RG32A), B/Florida/04/2006-like, and B/Malaysia/2506/2004-like vaccine strains. Absolute EC_{50}s were calculated using Graphpad Prism 5 and presented in Figure 2C. **(C)** FRIL MN against H1N1 X181 viruses produced in 9 day old embryonated chicken eggs (blue, egg-produced virus) and MDCK cells (magenta, cell-produced virus).

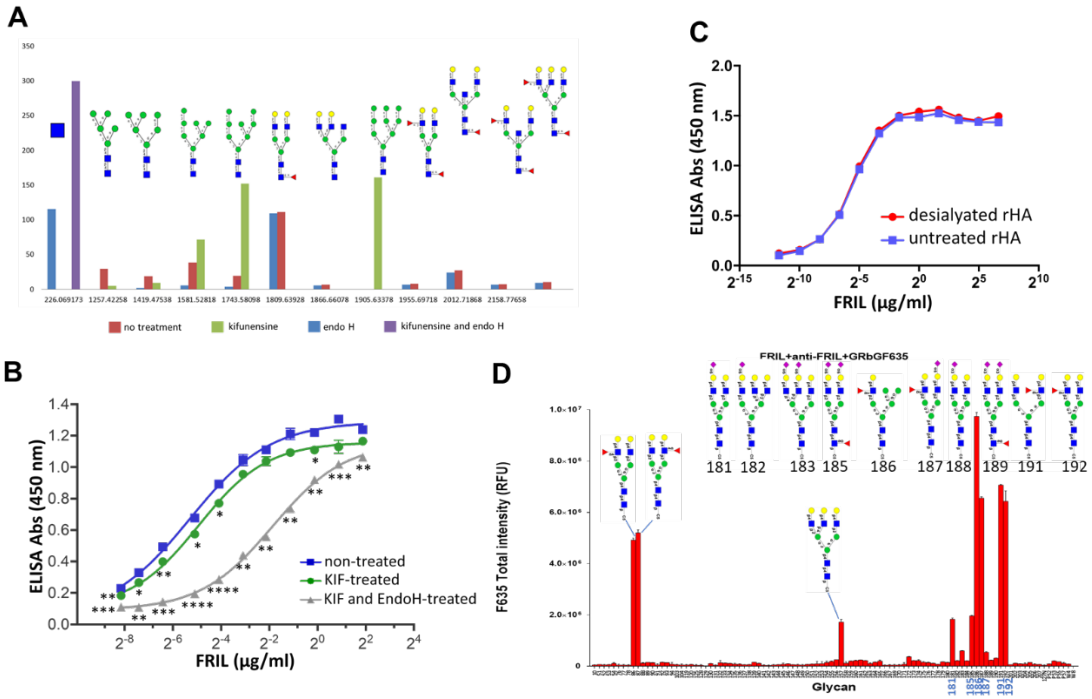

Figure S3. FRIL binds to complex type glycans, related to Figure 3. (A) Glycopeptide analysis of four different X181 virus particles produced from 9 day old embryonated eggs: no treatment (both complex and high mannose-type glycans exists on the virus surface naturally, red bars), mannosidase I inhibitor kifunensine treatment (high mannose only, green bars), endo H treatment (complex and a single GlcNAc on originally high mannose residues, blue bars) and kifunensine and endo H-treatment (only a single GlcNAc remains on each N-glycosylation site, purple bars). **(B)** Live virus ELISA where non-treated (blue), KIF-treated (green), and KIF- and endoH-treated (grey) purified H1N1 X181 particles were immobilized onto ELISA plates, then probed with FRIL and anti-FRIL antibodies **(C)** Recombinant A/California/7/2009 HA (rHA) produced from HEK293T cells, untreated (blue line) or with desialyation treatment (red line), were immobilized onto ELISA plates then probed with FRIL and anti-FRIL antibodies. Significance vs non-treated control was determined by 2-way ANOVA with Tukey's multiple comparison test (* p<0.05, ** p<0.01, *** p<0.001, **** p<0.0001) **(D)** FRIL microarray using anti-FRIL antibodies for detection instead of direct Cy3 labeling (as Fig. 3F). Symbol Nomenclature for Glycans (SNFG) was used to represent oligosaccharides on graph (blue square for GlcNAc, green circle for mannose, yellow circle for galactose, red triangle for fucose and purple diamond for NeuAc).

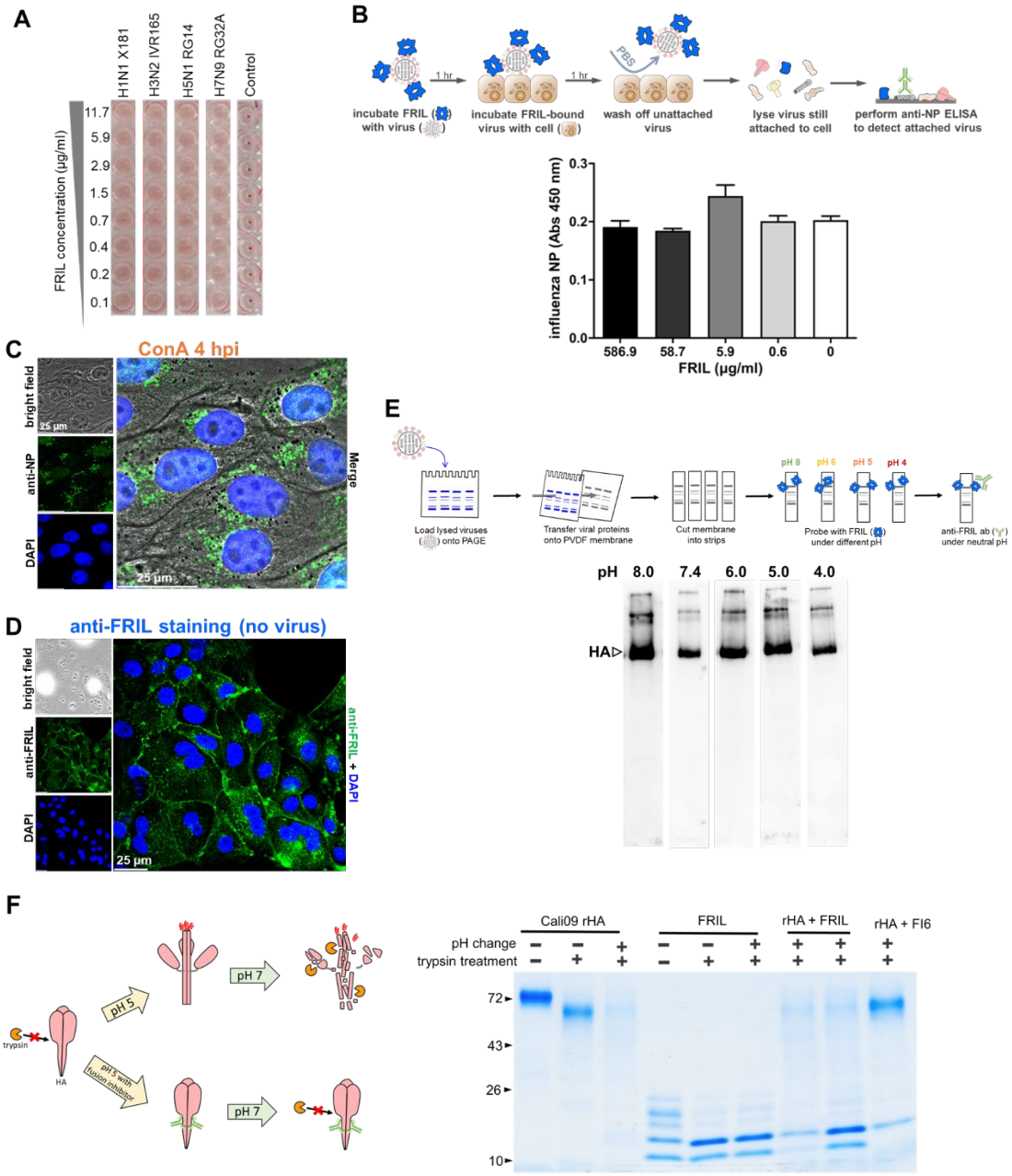

Figure S4. Effect of various treatments on FRIL binding, related to Figure 4. (A) HI of FRIL against 4 HAU/well of H1N1 X181, H3N2 IVR165, H5N1 RG14 and H7N9 RG32A. FRIL dilutions used in this assay were below FRIL's own HAU (14.4 μg/ml). **(B)** Schematic diagram of steps used in the determination of virus attachment to host cell by anti-NP ELISA. X181 virus particles were first incubated with different concentrations of FRIL for 1 hour, then layered onto MDCK cells. Unattached viruses were removed with three PBS washes, then the entire monolayer was lysed, releasing all cellular content (including NP on attached viruses). This protein mixture was dialyzed and plated onto a 96-well plate, and anti-NP ELISA was performed. **(C)** Results of the virus attachment anti-NP ELISA. FRIL did not inhibit X181 virus particle attachment to MDCK cells, even at 800 times its EC50 (0.74 μg/ml). **(D)** Immunofluorescence imaging of influenza RNP sequestered in late endosomes 4 hours post-infection after ConA treatment. **(E)** Immunofluorescence imaging of MDCK cell

interaction with FRIL (5 μg/ml) after 4 hours incubation. **(F)** (*upper panel*) Schematic diagram of FRIL immunoblotting under increasing acidity. FRIL was prepared in pH 8.0, 7.4, 6.0, 5.0 and 4.0 buffers and used to probe purified X181 virus particles lysed and blotted onto a PVDF membrane. Anti-FRIL primary and secondary antibodies were then added under neutral pH (pH 7.4). (*lower panel*) Result of FRIL immunoblotting with increasing acidity. All strips were subjected to the same exposure time. **(G)** (*left panel*) Schematic diagram of trypsin susceptibility assay steps. Under neutral pH, HA in its pre-fusion form is resistant to trypsin digestion. Lowering the pH to 5 causes HA to undergo a conformational change to initiate viral fusion with the endosomal membrane. The post-fusion conformation of HA is susceptible to trypsin digestion. A conformational change inhibitor, by inhibiting this pH-induced HA conformation change, would allow HA to remain in a pre-fusion trypsin-resistant state. (*right panel*) Results of the trypsin susceptibility assay. Recombinant HA (rHA) remained susceptible to trypsin digestion after pH change when FRIL was added in a 1:1 (lane 7) or 1:3 ratio (lane 8), in contrast to a 1:1 ratio of known fusion inhibitor FI6v3 (FI6, lane 9).

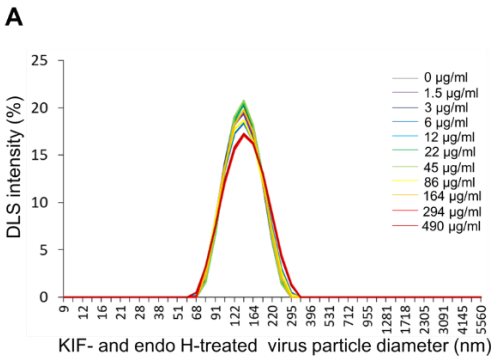

Figure S5. FRIL does not aggregate single GlcNAc influenza virion, related to Figure 5.

(A) Dynamic light scattering (DLS) analysis of kifunensine (KIF) and endoglycosidase H (endoH) treated virions (with a single GlcNAc per N-glycosylation site) under increasing concentrations of FRIL, from 1.5 µg/ml (13.38 nM) in purple line to 490 µg/ml (4.37 µM) in dark red line.

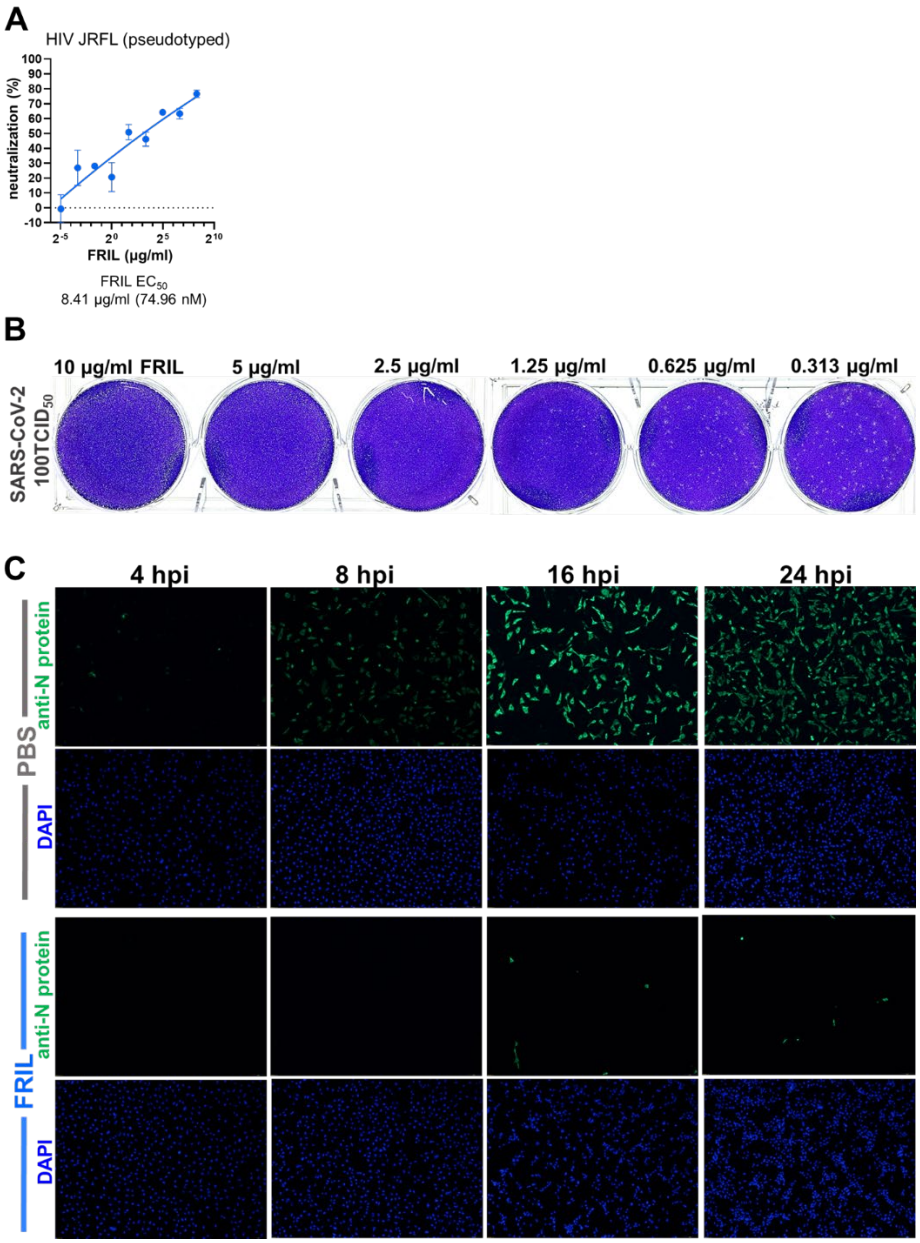

Figure S6. FRIL exhibits potent neutralization of SARS-CoV-2 but not HIV, related to Figure 6. **(A)** FRIL MN of HIV-1 JR-FL (pseudotyped) on TZM-bl cells, measured with a luciferase assay. **(B)** Raw image of FRIL plaque reduction assay with 100 $TCID_{50}$ of SARS-CoV-2 (BetaCoV/Taiwan/4/2020) (Fig 6B), from 10 μg/ml (89 nM) to 0.31 μg/ml (2.79 nM). Due to virus availability only one well per FRIL concentration was performed. **(C)** Raw image used for quantification of N protein positive cells at different time points after SARS-CoV-2 infection (Fig 6E). Data representative of 3 images.

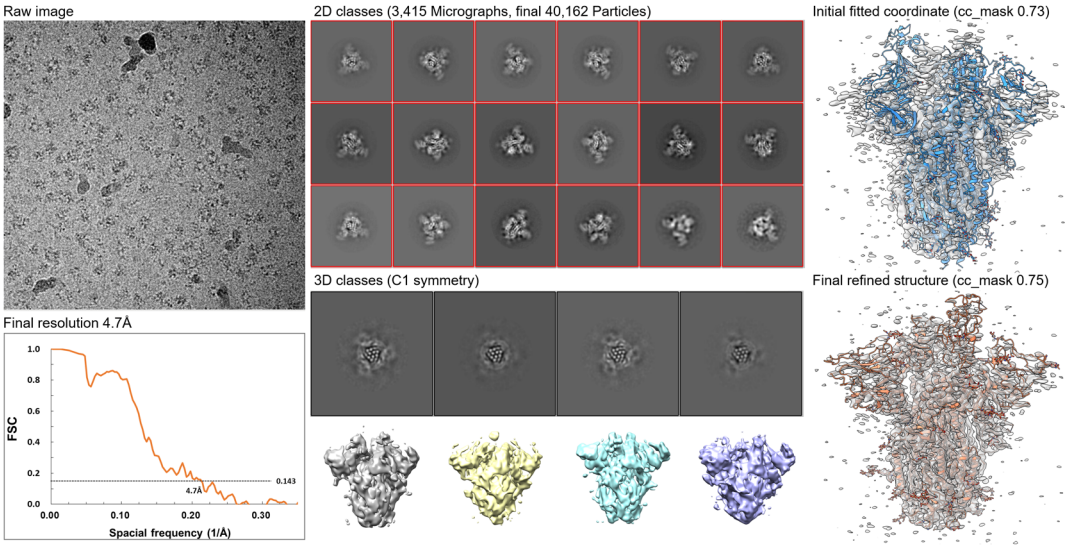

Figure S7. Cryo-EM structure of SARS-CoV-2 spike protein, related to Figure 7. 3,415 micrographs of HEK293-expressed fully glycosylated SARS-CoV-2 spike protein were collected at Academia Sinica Cryo-Electron Microscopy Center (ASCEM), Taiwan. A final set of 40,162 particles were selected for 3D reconstruction, resulted in a 4.7Å cryo-EM structure. Despite the relatively lower resolution than published spike structures (PDB 6VSB for example), the final refined structure has more residues in the loop region and extended glycan chains compared with 6VSB. CC_mask value increased about 0.02 with all the modifications. Further resolution improvement is ongoing.